JOURNAL OF MATERIALS SCIENCE 12 (1977) 1666–1672

The temperature and strain rate dependence of the flow stress of tantalum

K. G. HOGE
Energy Research and Development Administration, Washington, D.C., USA

A. K. MUKHERJEE
Department of Mechanical Engineering and Materials and Devices Research Group, University of California, Davis, California, USA

The temperature and strain rate dependence of the flow stress of tantalum was studied between 78 to 800 K at strain rates from 10^{-5} to 2×10^{4} sec^{-1}. The effect of temperature and strain rate on the lower yield stress can be explained by a model incorporating the combined operation of the Peierls mechanism and dislocation drag processes. The general behaviour of the stress–strain curve at various strain rates and temperatures is analysed in terms of a rate–temperature parameter.

1. Introduction

Recently considerable progress has been made in understanding the role of rate controlling dislocation mechanisms on the temperature and strain rate dependence of the flow stress of metals and alloys. At temperatures below that where diffusion-controlled mechanisms become operative, metals usually deform by thermally activated mechanisms. For a constant plastic strain rate, such mechanisms are characterized by rapidly decreasing flow stresses with increasing temperatures. The maximum temperature T_c over which these thermally activated mechanisms are operative depends on mechanistic details. For example, it increases with increasing activation energy and plastic strain rate.

At very high strain rates, stresses can be high enough to force dislocation mechanically past all barriers, unaided by thermal fluctuations. In this region viscous drag mechanisms are the controlling process for dislocation movement. The damping mechanisms first become rate controlling at a stress level, which depends on the magnitude of athermal stress, the total energy for thermal activation and the temperature. Experimental data indicate that in most metals this occurs when the plastic shear strain rate reaches a value of about 5×10^{3} sec^{-1}.

The principal objective of this report concerns rationalization of strain rate effects in metals over a large range of rates which encompass both thermally activated and drag mechanisms. Tantalum was chosen as the material for this investigation because its deformation is highly rate dependent, and also because sufficient information is available on the nature of the pertinent thermally activated deformation mechanisms. It is hoped that by combining the various dislocation processes into a single analytical model we will obtain a simple, yet complete, picture of the stress–strain rate–temperature relationship. Such a relationship would be useful for predicting the behaviour of a material at high strain rates from more easily obtainable low temperature and low rate data.

2. Experimental

Tests were conducted in tension and compression at strain rates from 10^{-5} to about 2×10^{4} sec^{-1}. Tests at rates below $10\,sec^{-1}$ were conducted on a hydraulically driven MTS universal test machine. Tests from 10 to $200\,sec^{-1}$ were run on a modified Dynapak metal working machine [1]. For tests at rates above 10^{-2} sec^{-1} strain was sensed by an Optron optical extensometer. Data was recorded on one oscilloscope as load and deformation versus time plots and on another as a load versus deformation trace.

For elevated temperature tests, specimens were

heated by a quartz lamp reflective lobe furnace. Low temperature tests used a Missimers temperature chamber for a first stage temperature drop to about 220 K. The second stage temperature drop was obtained by spraying liquid nitrogen into a secondary test chamber surrounding the specimen. Tests were conducted in the temperature range 78–800 K.

The Hopkinson split-bar technique [2, 3] was used for compression and tension tests at rates above 500 sec^{-1}. These tests were conducted at room temperature. Load versus time data was recorded on an oscilloscope.

Specimens were machined from a single rod of 99.9% fully recrystallized tantalum obtained from Kawecki–Berylco Industries. Compressive specimens were cylindrical; 1.02×10^{-2} m diameter and 0.76 to 1.52×10^{-2} m long. For tensile tests on the MTS and Dynapak machines, round specimens with a gauge section 3.18×10^{-2} m long and 0.64×10^{-2} m diameter were used. Specimens for Hopkinson split-bar tests has a gauge langth of 0.32 to 1.27×10^{-2} m and a diameter of 0.41×10^{-2} m.

3. Results and discusssion

3.1. Temperature dependence of flow stress

The temperature dependence of flow stress at a constant strain rate of 10^{-4} sec^{-1} is shown in Fig. 1. In the lower temperature region, the flow stress increases rapidly as the temperature is decreased indicating the operation of a thermally activated mechanism. Above some critical temperature (375 K) the behaviour becomes athermal. The total measured flow stress σ is the sum of the athermal component σ_A and the effective or thermally activated component σ^*. This analysis assumes that the athermal component is composed of long range internal back stresses, making the principal [12] of superposition applicable. The temperature dependence of σ_A parallels the temperature dependence of G, the shear modulus of elasticity [4]. Thus

$$\sigma_{A,T} = \sigma_{A,375}(G_T/G_{375}), \tag{1}$$

where the subscript refers to the absolute temperature.

3.2. Activation parameters

At low temperatures thermally activated dislocation mechanisms usually obey the empirical relationship suggested by the Boltzmann expression

$$\dot{\epsilon} = \dot{\epsilon}_0 \exp[-U(\sigma^*)]/kT, \tag{2}$$

where the activation energy U is a function of σ^*, k is the Boltzmann constant and T the absolute temperature. For some mechanisms, such as the intersection process [5], $U(\sigma^*)$ depends on the dislocation arrangements; for other processes, such as the Peierls [6–8], it is dependent of the substructure. The value of the pre-exponential factor $\dot{\epsilon}_0$ will always depend on the density of the mobile dislocation and will generally be insensitive to changes in temperature and stress.

The degree of the stress and strain dependence of the activation volume is often a definitive test for correlating the pertinent dislocation mechanism with the deformation phenomenon. This apparent activation volume v^* is defined by

$$\begin{aligned} v^* &= kT(\partial \ln \epsilon/\partial\sigma^*)_T \\ &= kT(\partial \ln \epsilon_0/\partial\sigma^*)_T - (\partial U/\partial\sigma^*)_T \\ &= -(\partial U/\partial\sigma^*)_T \end{aligned} \tag{3}$$

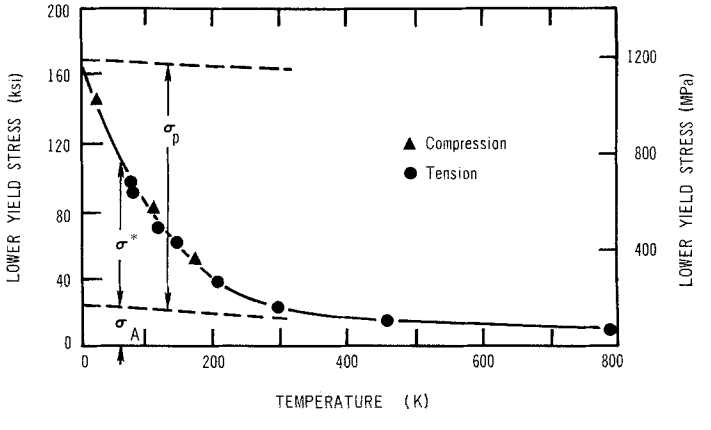

Figure 1 Effect of temperature on lower yield stress at a strain rate of 10^{-4} sec^{-1}.

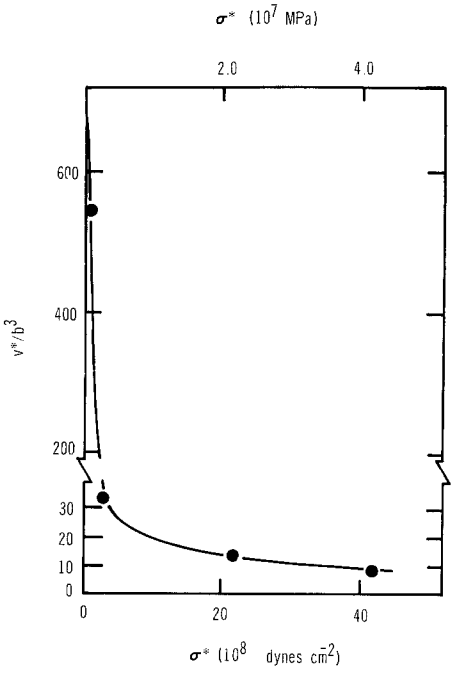

Figure 2 Activation volume versus thermally activated stress component.

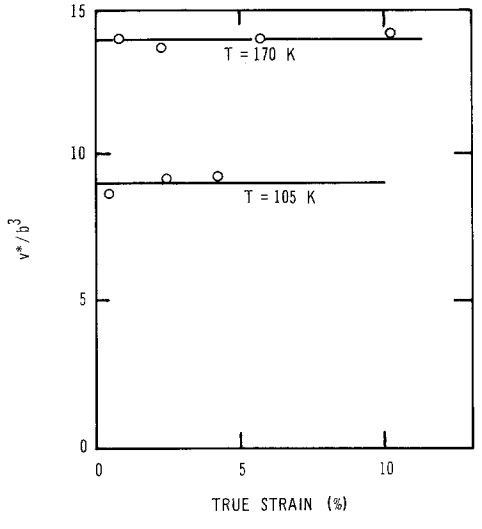

Figure 3 Activation volume versus strain.

The activation volume for deformation of bcc metals is in the range of 5 to 100 $\mathbf{b}^3$ ($\mathbf{b}$ = Burgers' vector) [9]. The activation volume of fcc ranges from 10 to 100 times larger. Furthermore, the activation volume of bcc metals is independent of strain while that for fcc metals decreases with increasing strain. The activation volumes calculated from the strain rate dependence of the flow stress at constant temperatures are shown in Fig. 2 as a function of effective stress. These activation volumes are much smaller than those obtained when the intersection mechanism is operative. The small values of the activation volume and the way they decrease with increasing values of σ^* are consistent with observations of earlier investigators, who correlated this type of behaviour with the operation of the Peierls' mechanism [9. 10].

Fig. 3 shows that activation volumes obtained at constant temperature are relatively independent of strain. These volumes were calculated from the response of stress to rapid changes in strain rate. If the intersection process were operative, the activation volume would decrease with increased straining. The lack of volume change constitutes additional confirmation that the Peierls' process is operative.

The above observations indicate that the Peierls' mechanism is rate controlling for the tantalum material reported in this paper. Next we will show how the experimental results can be correlated to the Peierls mechanism when the deformation is controlled by the rate of nucleation of pairs of kinks, as put forward by Dorn and Rajnak [8] and Guyot and Dorn [11]. We shall then try to expand the analysis to the region of very high strain rates where drag mechanisms contribute to the strain rate.

Using the Boltzmann approach, the rate of nucleation of a pair of kinks in a dislocation segment of length L is given by

$$\nu_n = \frac{\nu \mathbf{b} L}{2w^2} \exp(-U_n/kT), \qquad (4)$$

where ν is the Debye frequency, w is the width of a kink loop, U_n is the energy to nucleate a pair of kinks, k is the Boltzmann constant, T the absolute temperature and $\mathbf{b}$ the Burgers' vector. If a is the distance between Peierls valleys and ρ is the density, the average velocity of a dislocation moving as a result of nucleation is $\nu_n a$ and the average strain rate becomes

$$\dot{\epsilon} = \frac{\rho L a \mathbf{b}^2 \nu}{2w^2} \exp(-U_n/kT). \qquad (5)$$

At $T = T_c$ where σ^* first becomes zero, $U_n = 2U_k$ which equals the energy for a pair of kinks. Thus, for this condition

$$\dot{\epsilon} = \frac{\rho L a \mathbf{b}^2 \nu}{2w^2} \exp(-2U_k/kT_c). \qquad (6)$$

Therefore, for the same values of $\dot{\epsilon}$ and $\rho L/w$

$$\frac{U_n}{2U_k} = \frac{T}{T_c}. \tag{7}$$

Dorn and Rajnak calculated the critical value of U_n at any given temperature using the calculus of variations and numerical analysis [8].

$$\frac{\sigma^*}{\sigma_p} = f(U_n/2U_k) = f(T/T_c), \tag{8}$$

where the Peierls' stress at that temperature is

$$\sigma_p = \sigma_{p,0}(G_T/G_0). \tag{9}$$

The subscript 0 denotes values at absolute zero.

Our experimental data was analysed according to Equation 8 and plotted in Fig. 4. The theoretical relationship according to the Dorn–Rajnak model is also shown. Variations in the shape of the Peierls hill ($-1 \leqslant \alpha \leqslant 1$, where $\alpha = 0$ refers to sinusoidal hill) have only modest influence on the stress–strain rate relationship.

The theoretical stress dependence of the activation volume, where the latter is defined as

$$v^* = \frac{-\partial U}{\partial \sigma^*} = \frac{-2U_k \partial(U_n/2U_k)}{\sigma_p \partial(\sigma^*/\sigma_p)}, \tag{10}$$

is shown in Fig. 5. Again it can be seen that the experimental data points agree satisfactorily with the theoretical curves based on the Dorn–Rajnak Peierls model.

3.3. Flow stress–strain rate relation

In the very high strain rate region, viscous energy processes associated with dislocation drag play an important role. First it will be helpful to modify Equation 4. Guyot and Dorn [11] showed that, for a sinusoidal hill,

$$\frac{U_n}{2U_k} = \left(1 - \frac{\sigma^*}{\sigma_p}\right)^2. \tag{11}$$

Introducing Equation 11 into Equation 5 gives

$$\dot{\epsilon} = \frac{\rho L a \mathbf{b}^2 \nu}{2w^2} \exp\left[\frac{2U_k}{kT}\left(1 - \frac{\sigma^*}{\sigma_p}\right)^2\right]. \tag{12}$$

The various drag mechanisms that control the motion of dislocations at high strain rates have

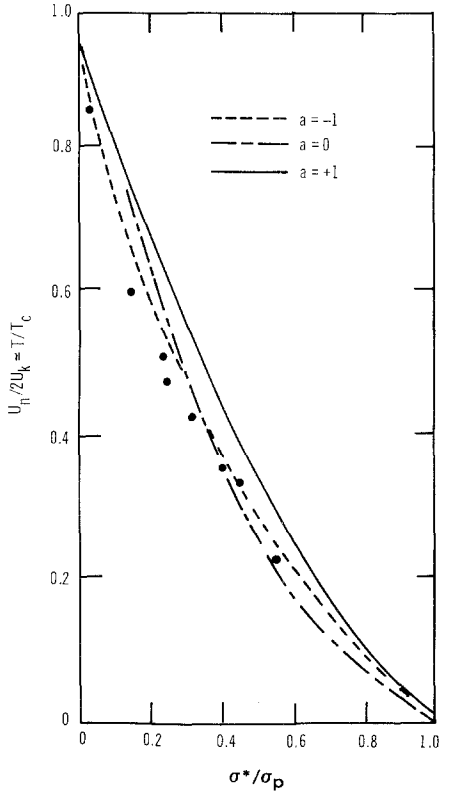

Figure 4 Energy to nucleate a pair of kinks as a function of stress.

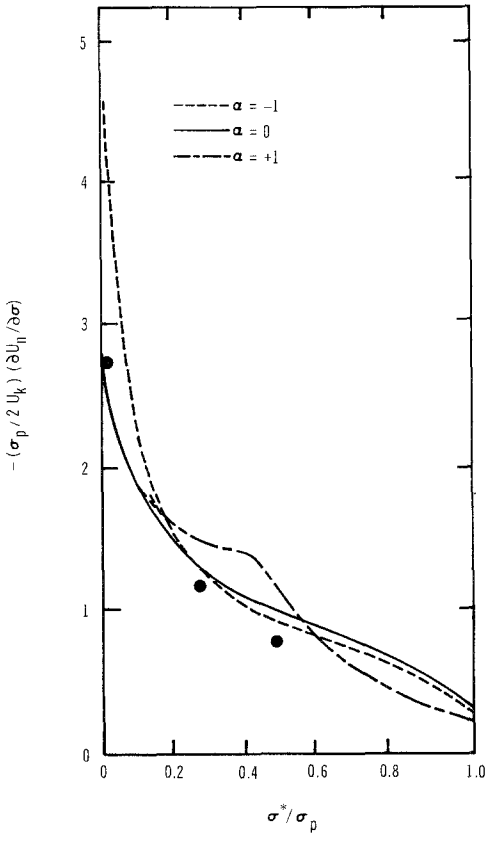

Figure 5 Activation volume versus thermally activated stress component.

been summarized by Klahn *et al.* [12]. These mechanisms are considered to be Newtonian. Consequently the drag force acting on a unit length of a moving dislocation is given by

$$\sigma^* \mathbf{b} = Ds, \tag{13}$$

where D is the net drag coefficient and s is the velocity of the dislocation. Since $\dot{\epsilon} = \rho \mathbf{b} s$, the strain rate for pure drag limited motion is

$$\dot{\epsilon} = \frac{\rho \mathbf{b}^2 \sigma}{D}. \tag{14}$$

To combine dislocation drag mechanisms with those for thermally activated passage of dislocations over Peierls' barrier, we will assume the total time for passage from hill to hill equals the time to pass a hill plus the time between hills where drag mechanisms are assumed operative. A more detailed and exact analysis [12, 13] of the thermally activated motion of dislocation overcoming localized obstacles and viscous drag mechanisms in a sequential process, reveal that the above assumption is an acceptable first approximation. Thus, the strain rate for the combined operation of drag and Peierls' mechanism is

$$\dot{\epsilon} = \frac{\rho \mathbf{b}^2}{\frac{2w^2}{Lav} \exp\left[\frac{2U_k}{kT}\left(1 - \left(\frac{\sigma^*}{\sigma_p}\right)^2\right)\right] + D/\sigma^*}. \tag{15}$$

The following values were used for evaluating Equation 15: $a \simeq \mathbf{b} = 2.86\,\text{Å} = 2.86 \times 10^{-10}$ m, $L/\mathbf{b} = 10^4$, $w/\mathbf{b} = 24$, $\nu = 10^{13}\,\text{sec}^{-1}$, $\rho = 10^3\,\text{m}^{-2}$, $U_k = 0.31\,\text{eV} = 0.05 \times 10^{-18}$ J. From the lower yield stress data in Fig. 1 we obtained

$$\sigma_p = 145\,\text{ksi} = 999.8\,\text{Mpa}$$

$$\sigma_A = 18\,\text{ksi} = 124.1\,\text{Mpa}$$

D was assumed [12] to equal 10^{-4} Mpa sec.

Experimental results of lower yield stress versus strain rate are shown in Fig. 6. The solid curve in Fig. 6 represents the theoretical relationship expressed by Equation 15. The experimental data and theoretical predictions show excellent agreement. The small amounts of disagreement noted lie within the experimental error of the tests. At strain rates less than $10^3\,\text{sec}^{-1}$, the drag mechanism does not contribute significantly to the flow stress and the results can also be analysed equally well by using Equation 12, which depicts the effect of Peierls' mechanism alone. But Equation 15, which incorporates the effects of dislocation drag as well, produces much better correlation in the high strain rate range. Preliminary results from experiments in progress in our laboratory on niobium at strain rates in excess of $8 \times 10^4\,\text{sec}^{-1}$ do support this point of view. Thus, the analysis based on the combined operation of Peierls' mechanism and dislocation drag processes appears valid.

Assuming that strain hardening is a function only of σ^* and σ_p, Equation 15 can be modified to provide a stress–strain temperature relationship. Taking the logarithm of both sides of Equation 15 and transposing, one obtains

$$T \log\left(\frac{\rho \mathbf{b}^2 Lav}{2w^2 \dot{\epsilon}} - \frac{DLav}{2w^2 \sigma^*}\right) = P. \tag{16}$$

P is a rate–temperature parameter that characterizes the flow behaviour. Since at strain rates below about $1000\,\text{sec}^{-1}$ dislocation drag processes contribute little, a simpler rate–temperature parameter can be obtained. Letting A equal the pre-exponential constant in Equation 12 and using the same mathematical manipulations as above,

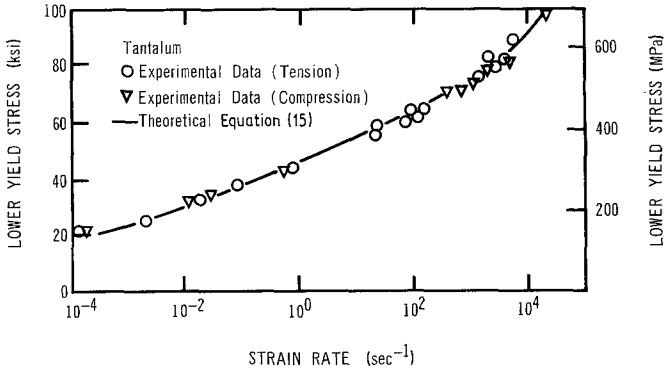

Figure 6 Experimental and theoretical results of lower yield stress versus strain rate at room temperature.

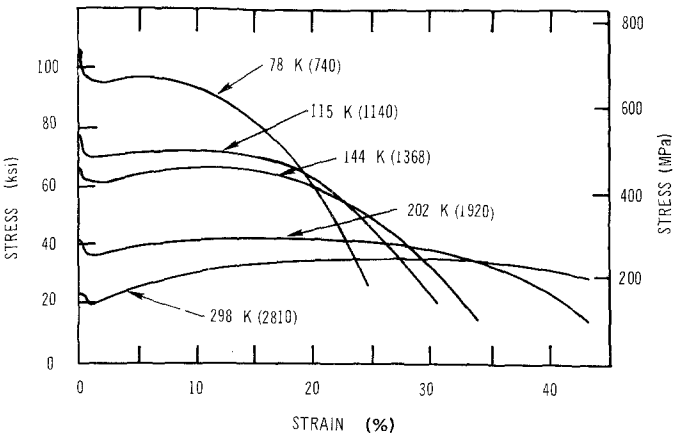

Figure 7 Effect of temperature on stress–strain behaviour. Tests were conducted at a strain rate of 10^{-4} sec^{-1}. Numbers in parentheses indicate values of P obtained from Equation 16.

one obtains

$$T \ln(A/\dot{\epsilon}) = \frac{2U_k}{2.3k}\left(1-\frac{\sigma^*}{\sigma_p}\right)^2 = P'. \quad (17)$$

Equation 16 or its simpler counterpart for low strain rate, Equation 17, predicts that tests conducted at various temperatures and rates should have similar stress–strain curves for equal values of P. Fig. 7 shows the stress–strain curves obtained at a strain rate of 10^{-4} sec^{-1} at various temperatures. Fig. 8 depicts stress–strain curves for tests performed at various rates at room temperature. The values for the parameter P, calculated from Equation 16, are shown in parentheses for each curve. Since curves with approximately equal P values are quite similar, this approach and the assumption that strain hardening is a function only of σ^* and σ_p appear to be valid. In addition, the variation in values of P with changes in strain rate and temperature closely approximates the corresponding change of ductility (as measured by fracture strain) with similar changes in strain rate and temperature. Thus, the parameter P appears useful in predicting the ductility that could be expected under some given combination of strain rate and temperature.

4. Conclusion

From this study of the temperature and strain rate dependence of the flow stress for polycrystalline tantalum it appears that:

(1) The rate controlling mechanism for deformation at low temperatures and strain rates can be rationalized in terms of a Peierls' mechanism. This conclusion was supported from the stress–temperature relationship and the variation of the activation volume with stress and strain.

(2) The room temperature flow stress–strain rate relation over extended range of strain rates can be explained satisfactorily by a model incorporating the combined operation of Peierls mechanism and dislocation drag mechanism.

(3) The nature of the stress–strain curve and the ductility at fracture can be explained in terms

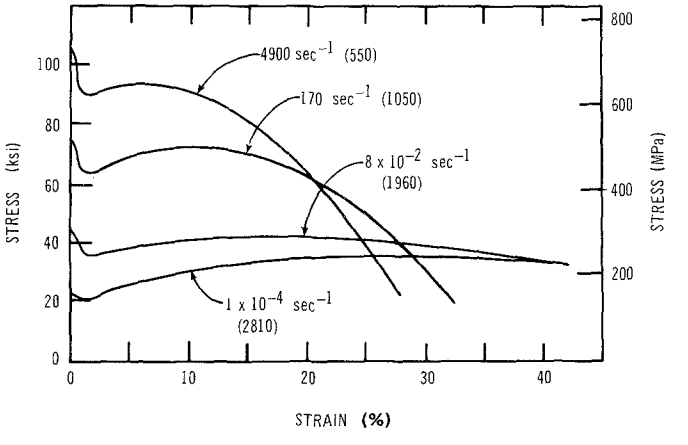

Figure 8 Effect of strain rate on stress–strain behaviour. Tests conducted at room temperature. Numbers in parentheses indicate values of P obtained from Equation 16.

of a rate–temperature parameter, assuming that strain hardening is a function of the Peierls' stress and the thermally activated component of the flow stress only and not a function of the rate of straining.

References

1. K. G. HOGE, *J. Basic Eng.* **88** (1966) 509.
2. F. E. HAUSER, *Exp. Mech.* **1** (1966) 395.
3. K. G. HOGE, *Explosivstoffe* **2** (1970) 39.
4. F. H. FEATHERSTONE, T. R. NEIGHBORS, *Phys. Rev.* **130** (1963) 1324.
5. H. CONRAD, Nat. Phys. Lab. Symposium on the Relation between Structure and Mechanical Properties of Metals, Teddington, England, 1963 (H.M.S.O., London, 1963) 475.
6. A. SEEGER, *Phil. Mag.* **1** (1956) 651.
7. V. CELLI, M. KABLER, T. NIMOIYA and R. THOMSON, *Phys. Rev.* **131** (1963) 58.
8. J. E. DORN and S. RAJNAK, *Trans. Met. Soc. AIME* **230** (1964) 1052.
9. S. S. LAU, S. RANJI, A. K. MUKHERJEE, G. THOMAS and J. E. DORN, *Acta. Met.* **15** (1967) 237.
10. R. T. SATO and A. K. MUKHERJEE, *Mater. Sci. Eng.* **8** (1971) 74.
11. P. GUYOT and J. E. DORN, *Can. J. Phys.* **45** (1967) 983.
12. D. KLAHN, A. K. MUKHERJEE and J. E. DORN, Proceedings of the second International Conference Strength of Metals and Alloys, Pacific Grove, California, 1970 vol. 3 (The American Society for Metals, 1970) p. 951.
13. J. F. DORN and A. K. MUKHERJEE, "Application of Rate Theory to Dislocation Dynamics", Lawrence Radiation Laboratory, University of California, Report No. UCRL-19097, October 1969; also presented as part of AIME Symposium on Thermal and Nonthermal Crystalline Deformation, Philadelphia, PA., October, 1969.

Received 30 January 1976 and accepted 17 January 1977.